

Microscale Materials Testing Using MEMS Actuators

M. A. Haque and M. T. A. Saif

Abstract—Small size scale and high resolutions in force and displacement measurements make MEMS actuators appropriate for micromechanical testing. In this paper, for the first time, we present methodologies for uniaxial tensile and cantilever bending testing of both micrometer- and submicrometer-scale freestanding specimens using MEMS actuators. We also introduce dry fabrication processes for the specimens. The methodologies allow freestanding single or multilayered thin-film specimens to be fabricated separately from the MEMS actuators. For the uniaxial tension test, tensile forces are applied by lateral comb drive actuators capable of generating a total load of $383\ \mu\text{N}$ at 40 V with resolutions on the order of 3 nN. A similar actuator is used in the bending test, with load resolution of 58 nN and spring constant of 0.78 N/m. The tensile testing methodology is demonstrated with the testing of a 110-nm-thick freestanding aluminum specimen. The cantilever bending experiment is performed on a 100-nm-thick aluminum specimen. The experimental setups can be mounted in a SEM (and also in a TEM after modifications for tensile testing) for *in situ* observation of materials behavior under different environmental conditions. Remarkable strengthening is observed in all the specimens tested compared to their bulk counterparts in both tensile and bending experiments. Experimental results highlight the potential of MEMS actuators as a new tool for materials research. [518]

Index Terms—Bending test, MEMS, tensile testing, thin films.

I. INTRODUCTION

THIN films at micrometer and submicrometer level are prevalently used in MEMS. They experience intrinsic loads developed during the deposition processes [13] and extrinsic loads due to operational and environmental conditions of the devices. They may fail to maintain mechanical integrity, as observed by cracking, delamination, and void/hillock formation under stresses [6]. Accurate prediction of thin-film materials response is a challenging problem because bulk testing methods, such as uniaxial tension test, are very difficult to apply directly to thin films, and extrapolation of bulk materials properties to the microscale is not scientific and reliable [15]. The problem is further complicated by the fact that mechanical properties of thin films are significantly affected by the fabrication processes [1] and are very sensitive to the influences of interfaces and adjoining materials [8].

Uniaxial tensile test, a popular method in bulk testing, is difficult to perform on thin films because of the challenges in 1) generating small forces (on the order of micronewtons), 2) gripping of the specimen, and 3) preventing bending force component in the specimen. While it is difficult to ensure no bending

during tests, the problems of fine force resolution and specimen gripping can be approached by using a substrate layer (usually very compliant, and with known materials properties) along with the actual film to be tested. This is demonstrated by [5], in which aluminum films were tested with thickness from 60 to 240 nm on polymer substrates. However, introduction of the substrate complicates the experimental analysis because: 1) the microscale materials properties of the substrate itself may not be known accurately and 2) the interface may influence the mechanical behavior of the film. Therefore, it is desirable to test freestanding thin films. This has been attempted by researchers who designed experimental setups with larger specimen sizes to cope with the coarser load resolutions. The tensiometer reported by Hoffman (1993) [7] is capable of generating 0.1-N force and was used to test $0.5 - 1.5\ \text{mm} \times 150\ \mu\text{m} \times 100\text{-nm}$ aluminum films. Ruud *et al.* [10] used motor-driven micrometers to produce elongation in freestanding films, then used a load cell to read the force and laser spots diffracted from the gratings on the specimen surface to determine the strain. The force resolution of their setup was 2 mN, and specimens could be tested with $1\ \text{cm} \times 3.3 - 0.013\ \text{mm} \times 1.9 - 2.6\ \mu\text{m}$ dimensions. Read [9] developed a piezoactuated tensile testing apparatus with force and displacement resolutions of $200\ \mu\text{N}$ and 20 nm, respectively, and demonstrated it on $700 \times 200 \times 1.2\ \mu\text{m}$ multilayered film specimens. Piezoelectric actuators have been previously utilized by [16] and [3], who used load cell-laser interferometry and strain gauge-optical encoder assemblies, respectively, to measure force and displacements. They tested polysilicon structures with thickness of 3.5 and $2\ \mu\text{m}$, respectively.

Cantilever bending test is also a popular bulk testing method and is equally difficult to implement on freestanding thin films. Since the bending stiffness of freestanding thin films is much smaller than their tensile stiffness, the force resolution of the loading device must be high, and its spring constant must be comparable to that of the specimen. The cantilever bending test was first applied to thin films by [17], who used a nanoindenter as the loading device. The thinnest freestanding film tested by this method was a $0.87\text{-}\mu\text{m}$ -thick gold film.

The motivation of this paper comes from the challenges involved with micromechanical testing and the opportunities offered by MEMS actuators. In this paper, we explore the effectiveness of MEMS actuators for uniaxial tensile and cantilever bending testing of thin films. The flexibility in the design for total force generation, force resolution, and structural compliance render MEMS actuators unique for the testing of micrometer- and submicrometer-level, freestanding, single- or multilayer thin films, or even films deposited on substrates, if required. Their small size and thermal and vacuum compatibility favor their application in experiments inside analytic chambers such as the SEM and TEM (with innovative stage design) under

Manuscript received January 4, 2000; revised November 30, 2000. This work was supported by the National Science Foundation under Career Grant ECS 97-34368. Subject Editor, R. T. Howe.

The authors are with the Department of Mechanical and Industrial Engineering, University of Illinois at Urbana-Champaign, Urbana, IL 61801 USA.

Publisher Item Identifier S 1057-7157(01)01593-1.

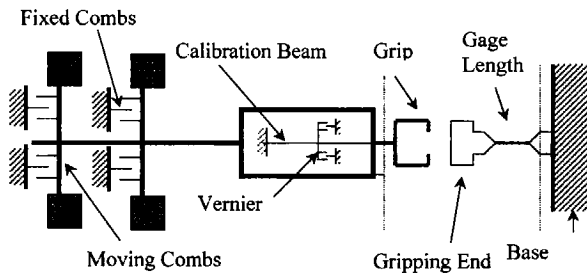


Fig. 1. Schematic of the tensile testing experimental setup. The actuator moves left upon actuation. The dashed lines indicate the cleaves in the substrates to make the actuator grip and specimen hang freely on air. The set of verniers are cofabricated with the actuator are used to measure its axial displacement.

different environmental conditions. In the next sections, we describe the experimental setups for tensile and bending testing to illustrate the potentials of MEMS actuators as mentioned above.

II. UNIAXIAL TENSILE TESTING METHODOLOGY

We have developed a MEMS-based tensile testing methodology to test freestanding films with thickness ranging from nanometers to micrometers. An electrostatic comb drive actuator generates the tensile force. The actuator is capable of gripping the specimen and has a self-calibration mechanism. The specimen is fabricated separately from the actuator and is designed to mesh with the actuator grip. We now present the methodology in detail.

Fig. 1 shows the schematic diagram of the tensile testing experimental setup. The actuator (shown on the left) has a C-shaped grip, a calibration beam made of single crystal silicon, and banks of fixed and movable combs. It spans an area of $3 \times 7 \text{ mm}^2$ and is $20 \text{ }\mu\text{m}$ deep. The backbone and the moving combs of the actuator are supported by structural beams. These beams are supported by anchors on the wafer and contribute to the actuators spring constant. The wafer is cut through the vertical dashed line so that the grip hangs freely in air. The specimen (shown in the right) has a freestanding gauge length section and a geometry that conforms to the actuator grip. The actuator and the specimen are mounted on precision motion stages to bring the specimen inside the actuator grip. This is done under an optical microscope. Once the specimen and actuator are aligned to each other, the whole experimental setup can be mounted inside a SEM to conduct *in situ* tests. The complete setup, shown in Fig. 2, occupies a space of $4 \text{ in} \times 1.5 \text{ in} \times 1.5 \text{ in}$, including the positioning stages. The size of the stages can be reduced further.

The force generated by a lateral electrostatic comb drive actuator is given by [14]

$$F = N\epsilon_0 \frac{h}{d} V^2 = \beta V^2 \quad (1)$$

where

- N number of moving and fixed comb pairs;
- ϵ_0 permittivity constant;
- h height of the combs;
- d lateral gap between the fixed and moving combs.

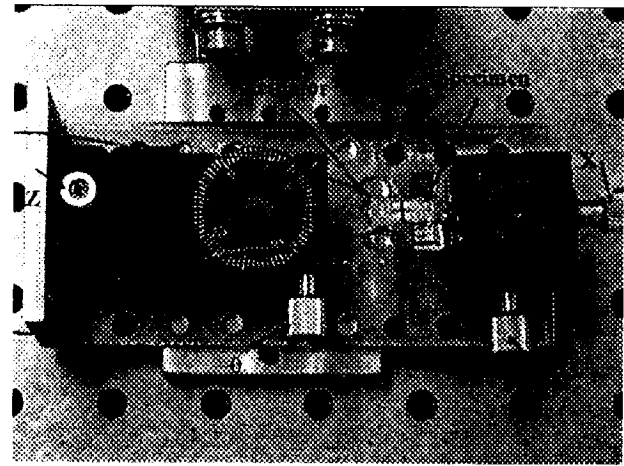


Fig. 2. Experimental setup. The actuator grip and the tensile test specimen are aligned by the precision positioning translation and rotational stages. This is done under an optical microscope.

These constants can be expressed as a unified constant β . After fabrication of the actuator, the actual dimensions of h and d vary from the design values. They also vary from actuator to actuator fabricated in the same wafer, rendering the constant β and the spring constant unknown. The calibration beam shown in Fig. 1 is used to determine these unknown parameters. It is a slender beam of single crystal silicon with known dimensions and material properties. One end of this beam is attached to the moving parts of the actuator, while the other one is fixed to an anchor. The actuator generates a compressive force on the beam and buckles it as the load exceeds a critical value P_{cr} that depends on the beam geometry and its elastic modulus. The lateral buckling displacement at different voltages, along with the dimensions of the beam, can be used to find the value of β and the spring constant of the actuator [11].

In a typical experiment, the wafer pieces containing the actuator and the specimen are mounted on positioning stages, as shown in Fig. 2. The gripping end of the specimen is then positioned inside the actuator grip with the stages. A rotational stage is used to align the actuator displacement direction to the tensile axis of the specimen. Initially, a small gap is left between the gripping edge of the specimen and the actuator grip. This gap, denoted by δ_0 , is about $1\text{--}2 \text{ }\mu\text{m}$ and prevents any preloading of the specimen. Voltage is then applied on the actuator. Upon actuation, the calibration beam absorbs all the force generated until its critical load (P_{cr}) is reached, after which the specimen and the actuator springs start to share the generated displacement and force. For an axial displacement δ ($\delta_0 \geq \delta$) of the actuator, the force balance is given by

$$\beta V^2 = k\delta + P_{cr} \left(1 + \frac{\delta}{2L}\right) \quad \text{for } \delta_0 \geq \delta \quad (2)$$

where

- V applied voltage;
- β calibration parameter defined in (1);
- k spring constant of the actuator;
- L length of the calibration beam.

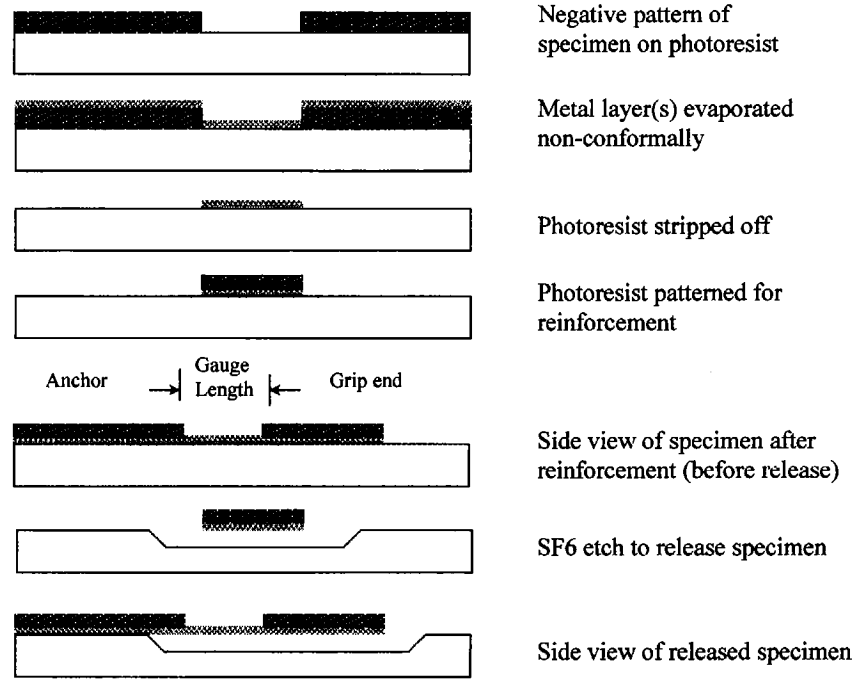


Fig. 3. Schematic of specimen fabrication process.

After the actuator is displaced by an amount of δ_0 , gripping of the specimen starts, and tensile force is applied on the specimen. The net force on the specimen F_s is given by

$$F_s = \beta V^2 - k\delta - P_{cr} \left(1 + \frac{\delta}{2L} \right), \quad \text{for } \delta \geq \delta_0. \quad (3)$$

For each value of applied voltage, the corresponding lateral displacement (D) of the calibration beam is measured with the help of cofabricated vernier scales (shown later in Fig. 5) that can read a change of D with $0.3 \mu\text{m}$ resolution under an optical microscope. The corresponding δ of the actuator is obtained from [11]

$$\delta = \frac{\pi^2 D^2}{4L}. \quad (4)$$

Once the axial displacement δ is obtained, the force on the specimen is then computed using (3). It is important to note that elongation of the specimen may not necessarily be restricted to the gauge length section. Therefore, the actual elongation in the specimen needs to be measured from the recorded digital images of the gauge length section under different applied forces. This was done using a software for dimension measurement, which has a pixel-to-pixel resolution of 90 nm . Resizing the acquired images before taking length measurements can further enhance this.

The force resolution of the actuator is obtained by differentiating (1)

$$dF = 2\beta V dV \quad (5)$$

which implies that the resolution changes with the applied voltage and depends on the resolution of the voltage source. The displacement resolution is obtained by differentiating (4), where we see that the lateral displacement of the calibration

beam is a magnified form of the axial displacement of the actuator. Therefore, the displacement resolution depends on the length of the calibration beam, as well as on the accuracy of reading of its lateral displacements. This is given by

$$d\delta = \frac{\pi^2 D}{2L} dD. \quad (6)$$

The force and displacement resolutions of the actuator used in this study are given later in this section. We now briefly describe the design and fabrication issues for the specimen and the actuator.

A. Design and Fabrication of the Specimen

The wet processing of freestanding films involves large surface forces, and hence films with submicrometer thickness are difficult to fabricate. Also, the specimen may be preloaded by these forces before the actual test. To avoid this problem, a dry process for specimen fabrication [4] was introduced.

Fig. 3 shows the schematic of the fabrication process. The process steps are as follows.

- 1) Photoresist AZ 5214 spun at 4000 rpm and soft-baked for 35 s at 100°C ;
- 2) Hard contact exposure with 65 mJ;
- 3) Postexposure bake for 45 s at 120°C ;
- 4) Flood exposure bake with 2 mJ/cm^2 energy flux for 10 s.
- 5) Development with 1:3 diluted AZ 351 developer for 45 s. At this stage, a negative pattern of the specimen is imprinted on the wafer with liftoff profile;
- 6) Evaporation of aluminum (more than one metal can be evaporated for multilayer specimens) on the pattern up to desired thickness (100 nm in this study);
- 7) Liftoff of the photoresist;
- 8) The specimen is then annealed at 200°C for 1 h. To prevent folding of the specimen at the gripping edges, we

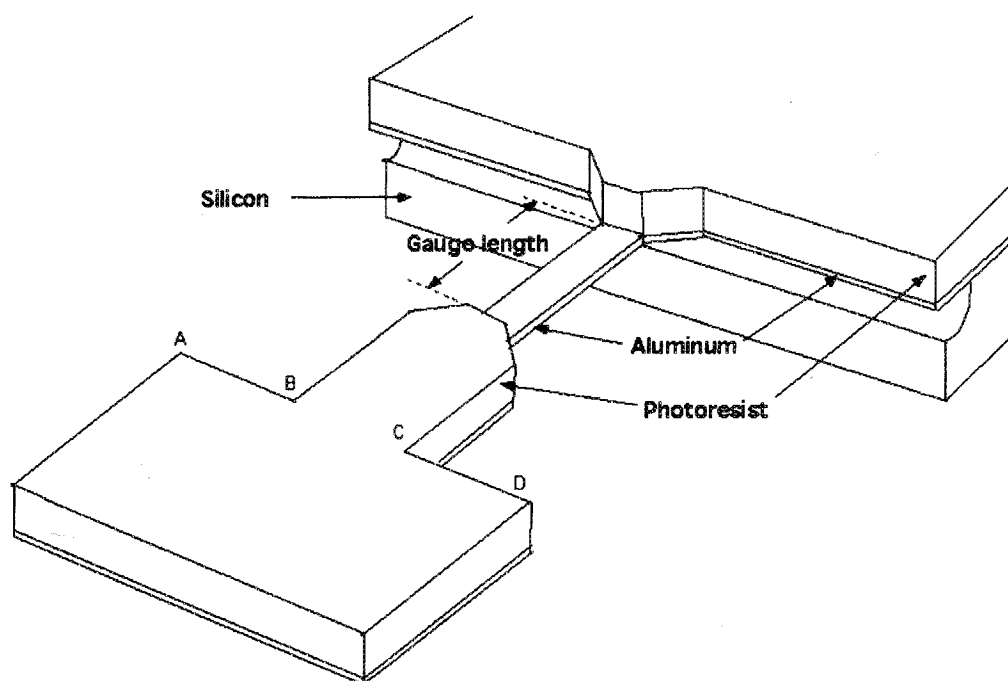


Fig. 4. Schematic of a freestanding tensile test specimen. The wafer is cleaved so that the gauge length section hangs freely on air. AB and CD are the gripping edges. The specimen is reinforced with a top layer of photoresist except for the gauge length section.

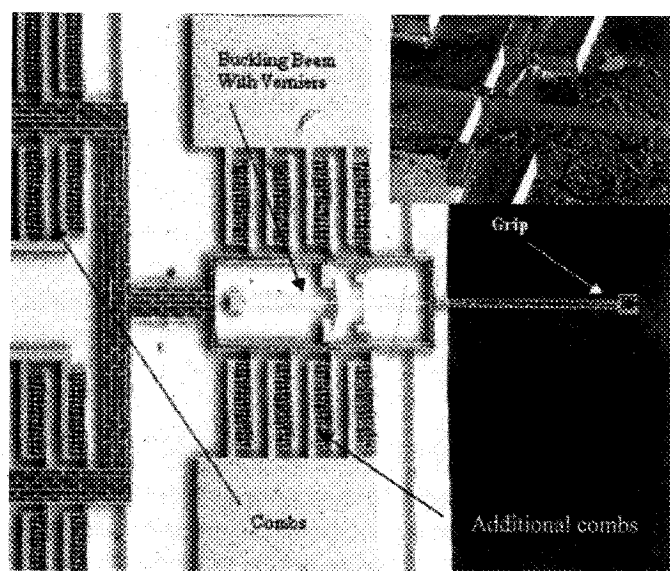


Fig. 5. The actuator showing the main combs, additional combs, calibration beam, and the grip (50 \times). Inset: vernier scale attached to the calibration beam.

reinforced the gripping end by patterning a layer of photoresist on the specimen excluding the gauge length section. We then evaporate 10 nm of aluminum onto the specimen, although this is not a required step in the fabrication process;

- 9) Reactive ion etching for 30 min at 50 mtorr pressure, 20 sccm SF_6 at 60 W to release the specimen.

Fig. 4 shows the schematic of a tensile testing specimen. The freestanding film is reinforced (everywhere except the gauge length section) by a layer of photoresist layer at its top. Distributed tensile load is applied by the actuator grip on the edges AB and CD.

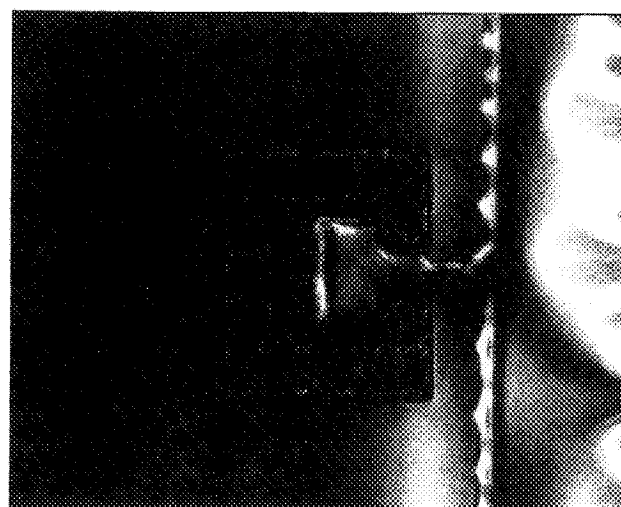


Fig. 6. A 110-nm-thick freestanding aluminum sample being gripped and stretched by the actuator.

B. Design and Fabrication of the Actuator

A lateral comb drive actuator with 3150 combs was designed to generate a total force of 382 μN at 40 V. In addition, there are 280 combs that can be separately activated for fine force resolution. The maximum allowable axial displacement of the actuator was 10 μm . Fig. 5 shows part of the actuator with the main and the additional combs and the calibration beam with the vernier scale. It was fabricated by a single crystal reactive ion etching and metallization process [12]. The calibration beam is 517 μm long, 1 μm wide, and 20 μm deep. The calibrated value of β is 0.228 $\mu\text{N}/\text{V}^2$ for the 3150 pairs of combs. The spring constant is 4.1 N/m.

The main set of 3150 comb pairs has a force resolution of 1.368 μN at 30 V for 0.1-V increments. The additional set of

Uniaxial Tension Test of 110 nm Aluminum Film

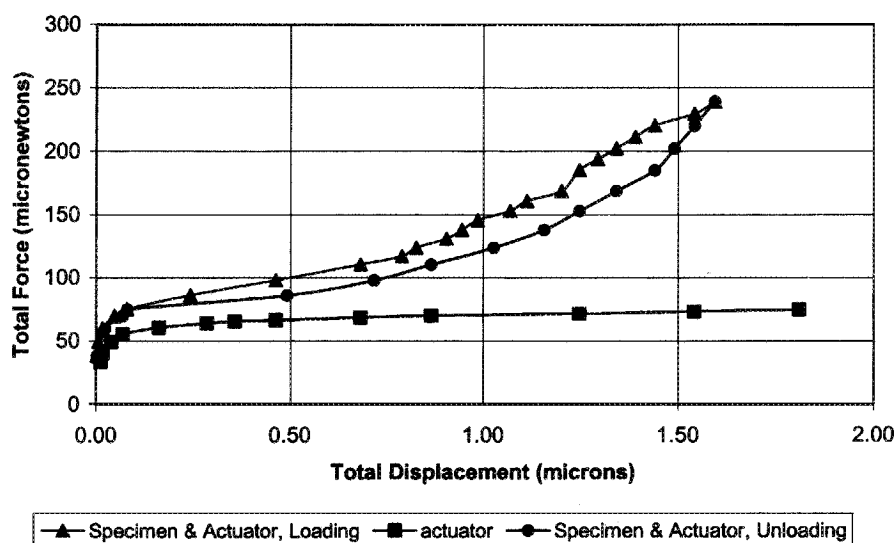


Fig. 7. Load-displacement plot for the 110-nm-thick aluminum film. Upper curves are for loading and unloading of both specimen and actuator. Lower curve shows load-displacement characteristics of the actuator only.

280 combs can provide 3-nN force resolution for an applied voltage of 1 V with a voltage source with 0.1 V resolution. The displacement resolution of the actuator is obtained from (6) and is 58 nm after 2 μm of axial displacement.

III. TENSILE TESTING RESULTS

To demonstrate the proposed methodology, we tested a specimen 2.3 μm wide with 10 μm gauge length and thickness of 110 nm made of >99.99% pure evaporated aluminum. The gripping end of the specimen was reinforced with a 1.3- μm -thick layer of photoresist, as shown in Fig. 4. Fig. 6 shows the specimen's being gripped and stretched by the actuator.

The force-displacement plots for loading and unloading of the aluminum film are given by the two upper curves in Fig. 8. The loads shown here are the amounts generated by the actuator as given by (1) and not just the loads on the specimen. The displacements shown in these curves include that of the actuator, as well as the gauge length and the gripping end of the specimen. Direct measurement of elongation in the gauge length section could not be performed under the optical microscope; hence the results are not expressed in terms of engineering strain. Due to intrinsic stress, the film was curled upwards after release from the substrate. Upon gripping and subsequent loading, it was first straightened, and hence it showed little resistance against displacement during this stage. After that, the specimen started to show resistance against deformation, as indicated by the change in the slopes of the load-displacement curve. Upon unloading, the specimen followed a different path, which indicates the occurrence of yielding in the specimen. The lower curve in Fig. 7 shows the load displacement characteristics of the actuator structure alone.

The results obtained in this study substantiate the feasibility of the proposed methodology and go beyond that. They provide

evidence of the difference of materials behavior in the macroscopic and microscopic scale. The aluminum film survived a tensile stress of roughly 616 MPa, which is higher than previously obtained values of about 180 MPa for freestanding films (Hoffman, 1993) [7] and 280 MPa [5] for 110- and 120-nm-thick aluminum films with polymer substrates, respectively. This behavior is significantly different from that the bulk pure aluminum with tensile strength of 55 MPa [2]. Conclusive results and fundamental understanding of the behavior of micrometer- and submicrometer-scale materials will require further studies under the SEM or the TEM and are beyond the scope of this paper.

IV. MICROCANTILEVER BENDING TESTING METHODOLOGY

The experimental setup for the microcantilever bending test consists of the microcantilever specimen, the MEMS actuator, and precision motion positioning stages to properly align the actuator with the specimen. We describe the setup components and the experimental procedure below.

1) *Specimen Preparation*: The specimen used in this study is a microcantilever aluminum beam of 99.99% purity. It is fabricated separately from the actuator. The beam is 11.3 μm long, 2.1 μm wide, and 100 nm thick. The fabrication process is basically the same as described for the tensile testing specimen in an earlier section.

2) *MEMS Actuator*: The actuator used in the microcantilever bending test has the same operating principles as described previously. It has a probe that applies a force on the cantilever beam specimen, as shown in Fig. 8. The actuator is 10 μm deep, spans an area of 2 mm \times 3 mm, and has a total of 660 combs. The β value of the actuator is 2.92×10^{-8} N/V². The actuator spring constant is 0.78 N/m. This value is comparable to the elastic spring constant of the specimen (0.38

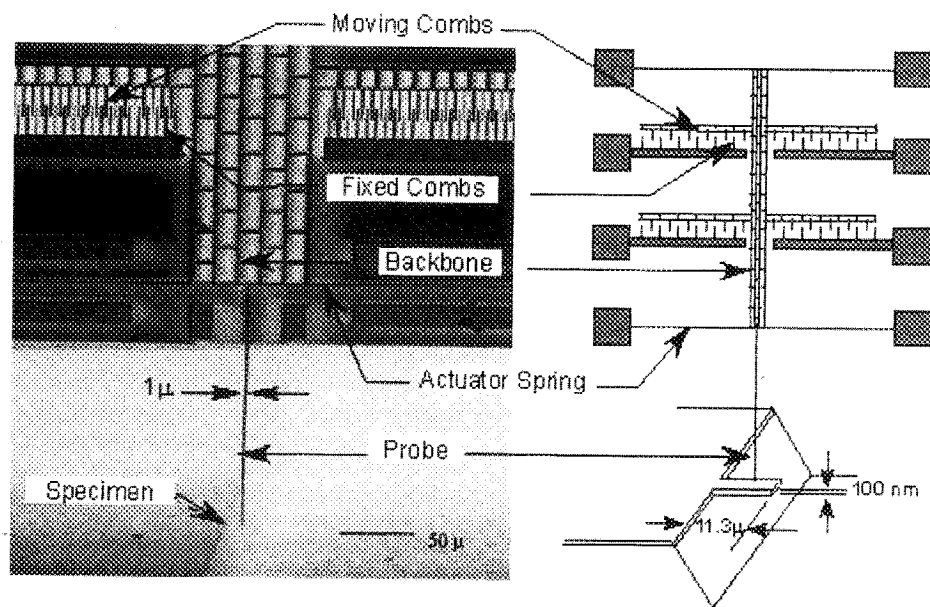


Fig. 8. SEM micrograph of the MEMS actuator and the microcantilever specimen after alignment. The actuator and the specimen are mounted on precision motion stages and then brought to the above configuration. The actuator probe motion is in the negative y direction only, applying bending load on the cantilever beam (barely visible at this magnification) at a constant lever arm. Right: schematic of the experimental setup.

N/m), which implies that the actuator springs are soft enough to capture the actual response of the beam to the bending load, and not just the data noise. The force resolution of the actuator is 58 nN at 10 V, assuming increments of 0.1 V.

After fabrication, the silicon substrate is cleaved such that the probe freely hangs in air. Precision motion stages were then used to align the actuator probe with the specimen, as shown in Fig. 8. At this stage, the lever arm of the cantilever beam is chosen to be $4.5 \mu\text{m}$ by positioning the actuator probe to the desired location along the length of the beam. Fig. 8 shows the SEM micrograph of the actuator with the probe after they are aligned. The specimen is barely visible at this magnification.

After alignment, an initial gap of about $1 \mu\text{m}$ was left between the specimen and actuator probe. Upon actuation, the probe approaches the specimen and applies force on it. It is important to note that the position of the actuator is fixed with respect to the specimen, so that the force is always applied to the specimen at a fixed lever arm. The contact point between the probe and the specimen moves along the length of the specimen during deformation.

For each value of the applied voltage, corresponding force on the specimen was calculated by determining the total force generated by the actuator and subtracting the restoring force. The deflections at the probe tip for each value of the applied load were acquired in form of digital images.

V. MICROCANTILEVER BENDING EXPERIMENTAL RESULTS

The microcantilever specimen was loaded and unloaded in two cycles. Fig. 9 shows the load-deflection profiles for these loading cycles. In this figure, several data points have been labeled with alphabets, which will be used to describe the results and analysis in this section. In the first cycle, loading was increased up to $0.75 \mu\text{N}$ (point D in Fig. 9). The initial nonlinearity (point A to B) is due to the unstable contact between the

Load-Deflection Profile for a 100 nm thick Al Film

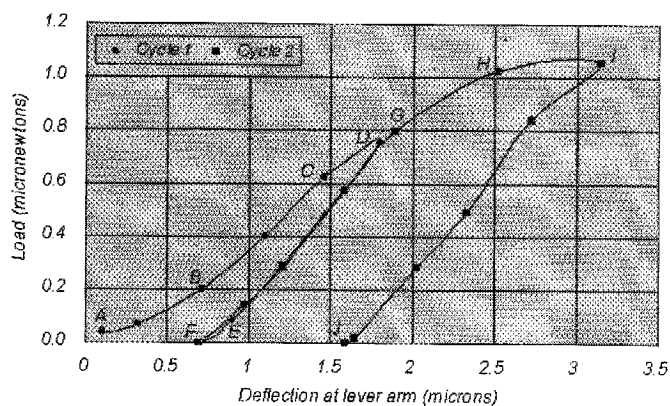


Fig. 9. Load-deflection profile of a 100-nm-thick aluminum microcantilever beam. Deflection measured at a lever arm of $4.5 \mu\text{m}$.

probe and the specimen and does not represent the true materials behavior. This is evident from the materials response in the rest of the loading and unloading history. This instability settles down and the beam deflects linearly with increasing load up to $0.62 \mu\text{N}$ (point C), when it just starts to show nonlinear response again. Upon unloading, the specimen behaves linearly (from point D to F) but shows some permanent deflection, indicating that plastic deformation has taken place. This permanent deflection was accounted for in determining the load-deflection profile for the next loading cycle. In this cycle, the specimen showed linear elastic behavior until $0.79 \mu\text{N}$ (point G) and then deviated from linearity. The load at point G is larger than that at point C, which reflects the strain hardening that occurred in the specimen. Once again, the specimen unloaded in a linear way and showed more plastic deformation when the probe was completely withdrawn from the specimen.

The stress on the specimen at the beam support is about 880 MPa for the loading point C where the film begins to yield. This

value is 49 times larger than the bulk yield stress of pure aluminum (55 MPa). The experimental results once again confirm the strengthening effect in thin films and incite further experimentation and analysis that are beyond the scope of this paper.

VI. CONCLUSION

We have demonstrated the potentials of MEMS actuators on micromechanical testing by performing uniaxial tensile test and microcantilever bending test on freestanding thin films in the micro- submicrometer-scale using MEMS devices. The attractive features of the proposed methodologies are:

- 1) flexibility in design for actuator force and displacement resolution;
- 2) easy dry fabrication of freestanding thin-film specimens with thickness ranging from micrometers to nanometers;
- 3) very small overall setup size encouraging in situ observation of materials behavior in analytical chambers such as the SEM and TEM.

Two tensile tests were carried out on polymer (photoresist) and aluminum films of thickness 1.3 μm and 110 nm, respectively. The results show significant difference in materials behavior between the bulk and microscales in uniaxial tension. Similar results are obtained from the microcantilever beam bending test on a 100-nm-thick aluminum film, where the yield stress is about 880 MPa, which is about 49 times the bulk yield stress for commercially pure aluminum.

ACKNOWLEDGMENT

The authors acknowledge C. Sager for his help during actuator fabrication. The actuators were fabricated in the Cornell NanoFabrication Facility at Cornell University. The specimens were fabricated in the Frederick Seitz Materials Research Laboratory at the University of Illinois at Urbana-Champaign.

REFERENCES

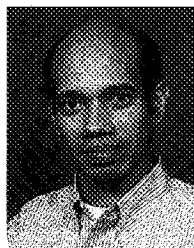
- [1] F. R. Brotzen, "Mechanical testing of thin films," *Int. Mater. Rev.*, vol. 39, no. 1, pp. 24–45, 1994.
- [2] W. D. Callister, *Materials Science and Engineering: An Introduction*, 4th ed. New York: Wiley, 1997.
- [3] S. Greek, F. Ericson, S. Johansson, and J. A. Schweitz, "Micromechanical tensile testing," in *Proc. Mater. Res. Soc. Symp.*, vol. 436, 1997, pp. 227–232.
- [4] M. A. Haque and M. T. A. Saif, "Investigation of micro-scale materials behavior with MEMS," in *Proc. Int. Mechanical Engineering Congress and Exposition*, Nashville, TN, 1999.
- [5] Y. S. Kang and P. S. Ho, "Thickness dependent mechanical behavior of submicron aluminum films," *J. Electr. Mater.*, vol. 26, no. 7, pp. 805–813, 1997.
- [6] M. Madou, *Fundamentals of Microfabrication*. Boca Raton, FL: CRC Press, 1997.

- [7] G. T. Mearini and R. W. Hoffman, "Tensile properties of aluminum/alumina multi-layered thin films," *J. Electron. Mater.*, vol. 22, no. 6, pp. 623–629, 1993.
- [8] W. D. Nix, "Mechanical properties of thin films," *Metallurgical Trans.*, vol. 20A, p. 2217, 1989.
- [9] D. T. Read, "Piezo-actuated microtensile test apparatus," *J. Testing Eval.*, vol. 26, no. 3, pp. 255–259, 1998.
- [10] J. A. Ruud, D. Josell, and F. Spaepen, "A new method for tensile testing of thin films," *J. Mater. Res.*, vol. 8, no. 1, pp. 112–117, 1993.
- [11] M. T. A. Saif and N. C. MacDonald, "Measurement of forces and spring constants of microinstruments," *Rev. Sci. Instrum.*, vol. 69, no. 3, pp. 1410–1422, Mar. 1998.
- [12] K. A. Shaw, Z. L. Zhang, and N. C. MacDonald, "SCREAM I: A single mask single-crystal silicon, reactive ion etching process for micro-electro-mechanical structures," *Sensors Actuators A*, vol. 40, 1994.
- [13] F. Spaepen and A. L. Shull, "Mechanical properties of thin films and multilayers," *Current Opinion Solid State Mater. Sci.*, vol. 1, pp. 679–683, 1996.
- [14] W. C. Tang, C. H. Nguyen, and R. T. Howe, "Laterally driven polysilicon resonant microstructures," *Sensors Actuators A*, vol. 20, pp. 25–32, 1989.
- [15] R. P. Vinci and J. J. Vlassak, "Mechanical behavior of thin films," in *Annu. Rev. Mater. Sci.*, vol. 26, 1996.
- [16] B. Yuan and W. N. Sharpe, "Mechanical testing of polysilicon thin films," *Exper. Mech.*, pp. 32–35, Mar./Apr. 1997.
- [17] T. P. Weihs, S. Hong, J. C. Bravman, and W. D. Nix, "Mechanical deflection of cantilever microbeams: A new technique for testing the mechanical properties of thin films," *J. Mater. Res.*, vol. 3, no. 5, pp. 931–942, 1988.



M. A. Haque received the B.S. and M.S. degrees in mechanical and industrial engineering, respectively, from Bangladesh University of Engineering & Technology, Bangladesh, in 1993 and 1995, respectively. He received the M.B.A. degree from the University of Alberta, Canada. He is currently pursuing the Ph.D. degree at the Department of Mechanical & Industrial Engineering, University of Illinois at Urbana-Champaign.

His research interests include micro/nanoscale materials science, design and fabrication of MEMS for microinstrumentation, and engineering optimization.



M. T. A. Saif received the B.S. degree in structural civil engineering from Bangladesh University of Engineering & Technology, Bangladesh, in 1984, the M.S. degree in structural civil engineering from Washington State University, Pullman, and the Ph.D. degree in theoretical and applied mechanics from Cornell University, Ithaca, NY, in 1993.

He was a Postdoctoral Associate in electrical engineering at Cornell University. He is currently an Assistant Professor in the Department of Mechanical & Industrial Engineering, University of Illinois at Urbana-Champaign. His research interests include design, analysis, and fabrication of MEMS for submicrometer-scale materials studies and noninvasive investigations of living cells; nonlinear dynamics of MEMS, and bistable MEMS sensors.